Am J Transl Res 2018;10(9):2796-2809
www.ajtr.org /ISSN:1943-8141/AJTR0079167

Original Article

Low-dose nicotine reduces the homing ability of murine BMSCs during fracture healing

Jing Zhang, Qilong Wan, Xin Yu, Gu Cheng, Yifeng Ni, Zubing Li

State Key Laboratory Breeding Base of Basic Science of Stomatology (Hubei-MOST) and Key Laboratory of Oral Biomedicine, Ministry of Education, School and Hospital of Stomatology and Department of Oral and Maxillofacial Trauma and Plastic Surgery, Wuhan University Stomatological Hospital, Wuhan University, Wuhan 430079, Hubei, China

Received May 7, 2018; Accepted August 7, 2018; Epub September 15, 2018; Published September 30, 2018

Abstract: Wound and fracture healing are affected by exposure to nicotine and other compounds in cigarettes. This study examined the effects of exposure to low-dose nicotine at sub-toxic concentrations on the proliferation, differentiation and migration of bone marrow stem cells (BMSCs) in vitro and their homing to fracture site in C57BL/6 mice. BMSCs were investigated in cells treated with or without nicotine (1 μM to 1 mM). Different concentrations of nicotine exhibited varied effects on BMSCs growth regulation and bone differentiation. CCK8 test significantly increased at a high nicotine concentration of 1 mM while calcium nodule staining with Alizarin red decreased at the same concentration. In vitro scratch test, Transwell tests and in vivo BMSCs homing tests showed negative effects on BMSCs migration at 10 μM to 1 mM nicotine test. Real-time PCR analysis revealed the down-regulation of SDF-1, CXCR4 and CXCR7, which were members of the potent chemotactic signaling system. Western blot analysis indicated the down-regulated expression levels of periostin expressed by nicotine-treated osteoblasts (1 μM to 100 μM). Micro CT results showed that nicotine delayed the fracture healing in mice. Our data suggest that exposure to low-dose nicotine concentrations may affect bone formation by inhibiting the migration and homing of BMSCs, which may be an important risk factor for bone healing delay in smoking patients.

Keywords: Bone fracture healing, BMSCs, nicotine, homing, migration

Introduction

Cigarette smoking is a powerful risk factor for severe health problem, including cancer, cardiovascular diseases and pulmonary diseases, and a serious medical concern worldwide [1], particularly in China, because of its high prevalence among male and even female adults [2]. Over the past decade, China has been the largest producer and consumer (40% of the global supply) of cigarettes [3, 4]. Numerous lines of evidence show that smoking is harmful to every organ in the body; specifically, smoking impairs wound and bone fracture healing in soft tissues [5]. Smoking affects oxygenation in tissues, serum concentrations of important growth factors, collagen synthesis and bone mineralization. Smoking is also associated with high risk of delayed bone union and high incidence of non-union [6]. Preoperative smoking cessation is an important measure that patients should undergo to improve surgical prognosis. However, smokers face difficulty in giving up smoking because of suddenness of injury and high rate of cigarette addiction. Moreover, the alteration of bone biology in smokers can persist even after smoking cessation for a long time, resulting in impaired fracture healing [7, 8]. Several lines of evidence indicate the harmful consequences of cigarette smoking on fracture healing. However, the mechanism of the smoking effect on fracture healing remains unclear, and few specific treatment options are available [9].

The chemical components of cigarette smoke are absolutely harmful on fracture healing and are rapidly absorbed and circulated in the human bloodstream [5, 9]. Nicotine is the main compound among the 4000 substances in cigarette smoke [10]. Studies indicate that nicotine negatively affects the survival and prolifer-

ation of cells and the mineralization capacity of osteoblasts and bone marrow stem cells (BMSCs). However, not all data suggested that nicotine is exclusively harmful to osteogenesis [11]. Scholars reported that nicotine exhibits bimodal effect on the proliferation and osteoblast differentiation of BMSCs. The differentiation and proliferation of osteoblasts are inhibited at high nicotine concentrations, whereas the differentiation and proliferation of pre-osteoblasts are enhanced at low nicotine concentrations [12]. Clinical studies indicated the low concentration of nicotine in smokers [11, 13]. The results of in vitro experiments may not appropriately explain the effect of nicotine on fracture healing. During fracture healing, BMSC homing is an important step for bone healing; however, few studies have investigated the mechanism through which nicotine affects bone healing [14]. Hence, we hypothesize that delayed bone healing in smokers is due to the effects of nicotine on the obstruction of the homing ability of BMSCs.

BMSCs are non-hematopoietic, multipotent stem cells that can differentiate into osteoblasts, chondrocytes, adipocytes, myoblasts and neurons [15]. During bone healing, BMSCs from local and distal bone marrow are attracted to wounded sites by chemotactic factor and differentiate into osteoblasts [16]. BMSCs are an important source of osteoblasts during fracture healing and are often used in facilitating fracture healing [17], while inhibiting the migration of BMSCs affects wound healing [18]. It's reported that nicotine inhibits cell migration during wound healing [19]. However, the effect of nicotine on BMSC migration has been rarely investigated. Thus, we speculate that nicotine may affect BMSC homing during bone healing.

This study aims to investigate the effect of nicotine on BMSC migration in vivo and in vitro. The proliferation and differentiation of BMSCs and protein and signaling pathways through which nicotine affects the migration and homing of BMSCs are also evaluated.

Materials and methods

Isolation and culture of murine BMSCs

All animal experiments were carried out in accordance with the protocols authorized by Wuhan University's Animal Care and Use Committee. The BMSCs of mice were collected from 4 weeks age old green fluorescent protein (GFP) transgenic mice (C57BL/6-Tg[UBC-GFP]0Scha/J) as previously described [20]. After anesthetized briefly in a CO_2 chamber, the femurs of the mice were carefully exposed and cut at both metaphyseal ends. Then, the bone marrow was flushed out with DMEM (Hyclone, Logan, Utah) containing 10% FBS (Gibco, NY) and 100 U/mL of streptomycin and penicillin (Hyclone). After repeated pipetting, the bone marrow mixture was centrifuged at 1000 g for 5 min, resuspended in fresh complete medium, seeded on culture flasks, and then incubated at 37°C, 5% CO_2. After being cultured for 2 days, nonadherent cells were removed. After reaching 80-100% confluence, the cells were detached with 0.25% Trypsin (Hyclone), and the cells were subcultured into new culture flasks subsequently. Only passage 1 cells were used in the following experiments of this study.

Cell culture

MC3T3-E1 cell line (Subclone 15) was purchased from China Center for Type Culture Collection (Wuhan, China). Cells were routinely cultured in α-MEM (Hyclone) containing with 10% FBS (Gibco) and 1% Penicillin and Streptomycin (Hyclone).

Alizarin red assay

For the measurement of cell differentiation, cells were seeded into 12-well plates and cultured to sub confluence in complete medium which was then replaced by osteogenic medium that consists of α-MEM, 10% FBS, 1% penicillin and streptomycin, 50 mg/ml ascorbic acid and 10 mM β-glycerophosphate. After 21 days culture with the medium refreshed thrice a week, cells were fixed with 95% ethanol, and stained as previously described [21]. The stained portions were photographed with a digital camera and inverted microscope. The pigmented mineralized nodules were subsequently dissolved with Cetylpyridinium Chloride (Sigma-Aldrich) separately and optical density at 562 nm (OD520 nm) was measured.

Cell proliferation assay

For the measurement of cell proliferation, the cells were cultured in 96-well plates. After the cells reached sub-confluence, FBS concentra-

Table 1. Oligonucleotides used for RT-PCR

Specificity	Sequence
SDF-1	Forward: 5'-GAGAGCCACATCGCCAGAG-3'
	Reverse: 5'-TTTCGGGTCAATGCACACTTG-3'
CXCR4	Forward: 5'-AAAGCTAGCCGTGATCCTCA-3'
	Reverse: 5'-CACCATTTCAGGCTTTGGTT-3'
CXCR7	Forward: 5'-TCACCTACTTCACCGGCACC-3'
	Reverse: 5'-ACATGGCTCTAGCGAGCAGG-3'
MMP-8	Forward: 5'-GGTATTGGAGGAGATGCT C-3'
	Reverse: 5'-GGCTTGGACACTCCTTGG-3'
MMP-13	Forward: 5'-GGTCCCAAACGAACTTAACTTACA-3'
	Reverse: 5'-CCTTGAACGTCATCAGGAAGC-3'
GAPDH	Forward: 5'-ACCACAGTCCATGCCATCAC-3'
	Reverse: 5'-TCCACCACCCTGTTGCTGTA-3'

tion was reduced to 1%. Cell numbers were measured using a CCK-8 kit (Dojindo, Mashikimachi, Japan) following the manufacturer's instructions on days 0, 1, 3, and 7.

Cell migration assay

For the measurement of BMSCs migration, BMSCs were seeded into the upper chamber of the Costar Transwell inserts (#3422, pore size, 8 μm) (Corning) at a density of 1.0×10^4 cells/well. After incubation for 12 h at 37°C, the cells in the upper chamber were carefully removed using cotton swab. The permeable cells were fixed in 4% paraformaldehyde (PFA) and stained with crystal violet. Then, cells were photographed and quantified using Image Pro Plus 6.0 software.

The scratch test

Cells of each group were seeded into a 12-well plate (Corning), when the degree of fusion reached 80-90%, a wound was created along the bottom of the plate with 1 mM scratch pen; cells were slightly washed once with PBS, and then incubated with serum-free medium. Cell movement in 24 h was observed under inverted microscope and photographed; distance of the change in the wound was recorded to show the migration rate.

Total RNA extraction and quantitative real-time PCR (qPCR) analysis

For qPCR, cells were seeded in 12-well plates (Corning). Samples were washed with PBS for three times, total RNA was extracted using EZNA total RNA kit (Omega, Norcross, GA) according to the manufacturer's protocol, 1 μg RNA templates were reverse-transcribed into cDNA using First Strand cDNA Synthesis Kit (Thermo, Waltham, MA). qPCR was performed on Bio-Rad CFX 96 real-time PCR machine using the All-in-One™ qPCR Mix (Thermo) following the manufacturer's protocol. Primers were designed according to published literature (**Table 1**) [22-25]. Expression of migration markers were examined, including stromal cell-derived factor 1 (SDF-1), chemokine receptor type 4 (CXCR4), CXCR7, matrix metalloproteinase 8 (MMP-8) and MMP-13. All values were normalized to GAPDH and analyzed using ΔCt method.

Total protein extraction and western blot

For Western blot, cells were seeded in 3.5 cm flask (Corning) and grew to confluence. Total cellular protein was prepared by lysing cells with RIPA (Thermo) supplemented with 1% PMSF (Roche, Basel, Switzerland). The concentration of the total protein was assessed using Pierce™ BCA Protein Assay Kit (Thermo). Then 20 μg protein samples were separated by SDS-PAGE, and transferred to a PVDF membrane (Roche) by electro blotting. After blocking with 5% milk, membranes were incubated overnight on a shaker at 4°C with one of the following antibodies: Anti-periostin (POSTN) (Abcam, Cambridge, MA), anti-GAPDH (Abcam), and anti-Collagen I (Abcam). The membranes were then incubated with a secondary antibody, including HRP-conjugated goat-anti-rabbit IgG (Abcam). GAPDH was used as the internal reference.

Bone tissue culture

For bone tissue culture, flesh femurs from 6-week-old male C57BL/6 mice were prepared as mentioned above and bone marrow was removed by repeatedly flushing with PBS for three times. The middle femur bone segments (5 mm) were used and cut longitudinally to expose the medullary side. Effects of living bone with or without nicotine (100 μM) versus devitalized bone (upon boiling) segments were then determined by culturing bone segments with GFP-BMSCs in culture dishes for 7 days. Culture media were changed every 3 days.

Animal models and operational treatments

All animals in this study were treated according to internationally recognized guidelines on ani-

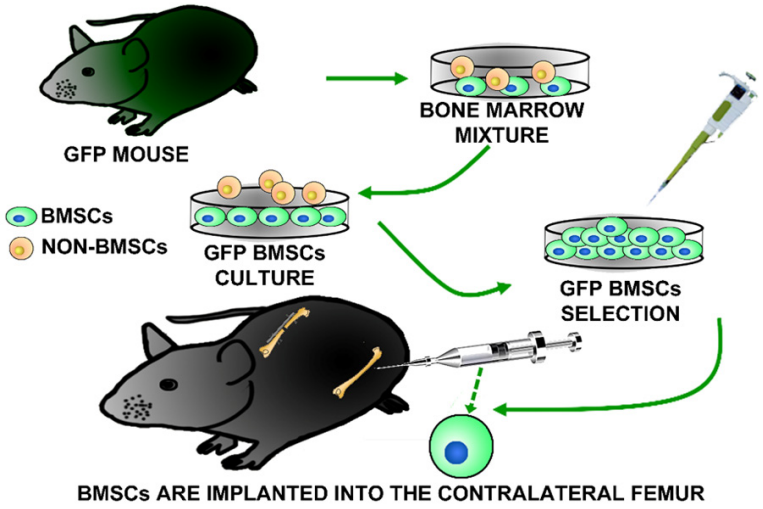

Figure 1. Schematic diagram representing the steps used to transplant BMSCs into the murine fracture model. The bone marrow collected from 4 weeks age old GFP mice was flushed out with complete medium, and then seeded on culture flasks. After being cultured for 2 days, nonadherent cells were removed and BMSCs were subcultured into new culture flasks subsequently. Mouse left femoral segmental defects (1.2 mm) were established while about $1*10^5$ GFP BMSCs were suspended in 20 μL of PBS and then injected into the contralateral femoral marrow cavity of fracture site with a microinjector.

mal welfare and with the approval of the Medical Ethics Committee of Hospital of Stomatology, Wuhan University. 36 6-week-old male mice purchased from Hubei Provincial Laboratory Animal Center and bred at the SPF Animal Lab of Wuhan University Stomatology School were divided into four groups of 6 mice each, two of them were considered nicotine groups (test A, test B and test C) and two were used as control groups (control A, control B and control C). Nicotine hemisphere (Sigma. Louis, MO, USA) was diluted in saline at the concentration of 5 mg/ml for the experimental groups. Each mouse received a volume of the diluted solution subcutaneous injection calculated as 3 mg/kg b.i.d according to the procedure proposed by Saito et al. [26]. The control groups received saline under the same conditions as the test groups. All animals received either nicotine or saline from 1 week before surgery until sacrifice for test. None mouse died by accident intraoperation or postoperation. Mouse left femoral segmental defects (1.2 mm) were established according to our previously published protocols [21]. Then, two needles were inserted into the bone cavity at both ends of the right femur. Saline was injected from one syringe to the marrow cavity, while the bone marrow-saline mixture was drawn out gently by pumping on the other syringe for three times to clear the bone marrow cavity. $1*10^5$ BMSCs from the GFP mice were suspended in 20 μL of phosphate-buffered saline and then injected into the marrow cavity through one needle with a microinjector. The needle holes were sealed with bone wax after the surgery (**Figure 1**). Test A and control A were applied in In vivo small animal imaging 7 days after the surgery; test B/control B and test C/control C were euthanasia by narcotic overdose anesthesia for Micro-computed tomography (μ-CT) analysis at 2 weeks and 5 weeks post-surgery.

In vivo small animal imaging

In all transplanted mice, homing of viable GFP+ BMSC was analyzed with a non-invasive in vivo small animal imaging system (PE Spectrum & Quantum FX, PerkinElmer USA), 1 week post-surgery. After the mice were anesthetized, GFP signals were recorded for at least 1 min. Fluorescence signal recordings were layered onto an X-ray image to create composite Fluorescence-X-ray images for location. Then the animals were sacrifice for the histology test next.

μ-CT analysis

Femora were flushed using running water for 24 h after 4% PFA fixation, then embedded in paraffin. The fixation devices were carefully removed. The paraffin-embedded samples were scanned using a μ-CT 50 imaging system (Scanco Medical AG, Bassersdorf, Switherland). The X-ray tube was set at 70 kV, 85 mA with the resolution was 20 μm (Integration time = 400 ms) paralleling the axis of the femora. Analysis and three-dimensional (3D) reconstruction were performed using the software provided by the manufacturer.

Histology and immunofluorescence staining

Following fixation, the samples underwent decalcification, dehydration, waxing and embed-

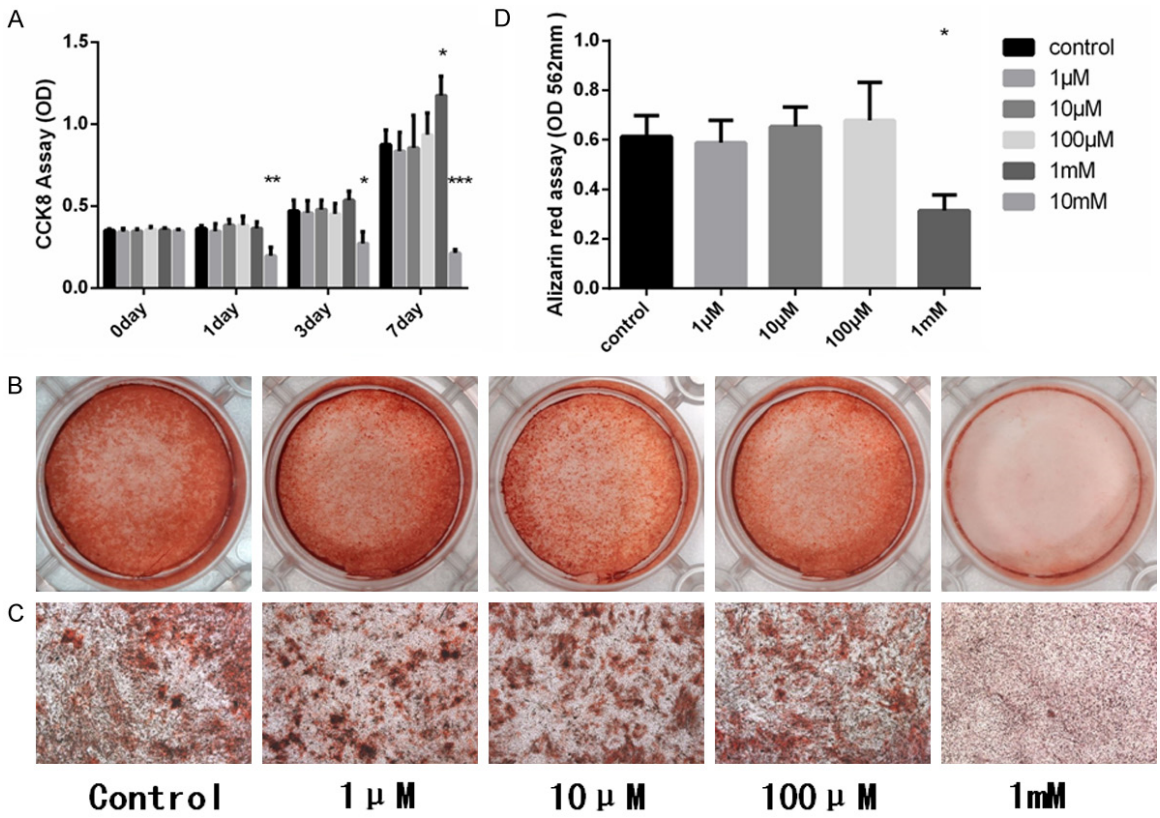

Figure 2. BMSCs were cultured with nicotine. A. The effect of nicotine on proliferation was assessed by CCK8 assay at 0, 1, 3, and 7 days with 1 μM-10 mM nicotine. B. BMSCs were cultured with 1 μM-1 mM nicotine for 21 days to test the effect of nicotine on calcium accumulation. The stained portions were photographed with a digital camera. C. Microscopic images were obtained using the Nikon inverted microscope. (original magnification 50 ×). D. The stained portion was dissolved using Cetylpyridinium Chlorid solution, and optical density was then measured. When cultured in media containing 1 mM nicotine, calcium accumulation decreased significantly. Data shown are the means ± SD for 3 independent experiments. *P < 0.05, **P < 0.05, ***P < 0.001 compared to the control group treated without nicotine.

ding. The fixation devices were then carefully removed from the paraffin-embedded samples, and the voids left were resealed with paraffin. Samples were sliced into 5 μm-thick longitudinal serial sections and then subjected to immunofluorescence staining with anti-GFP (Abcam) according to our previous research protocol [27].

Data analysis

For all quantitative data, analysis of variance (ANOVA) was employed to evaluate the effect of one variable on two or more independent groups. In the event of a two-group effect, individual pairs of means were compared using the t-test. Data were calculated as mean ± standard deviation, and in some cases, converted to percent of control. A value of $P < 0.05$ was used to determine whether differences were statistically significant.

Result

Effect of nicotine on proliferation and differentiation of BMSCs

BMSCs were treated with various concentrations of nicotine (1 μM-10 mM), and the effect on proliferation was analyzed using the CCK8 assay. On day 1, the cell viability of BMSCs treated with nicotine at concentrations between 1 μM and 1 mM was not different from that of the controls. While, the viability of cells decreased significantly when they were treated with 10 mM nicotine ($P < 0.05$) at all the time point. On day 3, BMSCs cultured with nicotine concentrations of 1 μM and 1 mM showed a similar situation as day 1. Also, the survival of BMSCs incubated with 10 mM nicotine was significantly decreased ($P < 0.05$). On day 7, BMSCs cultured with 1 mM nicotine showed increased proliferation, while those cultured

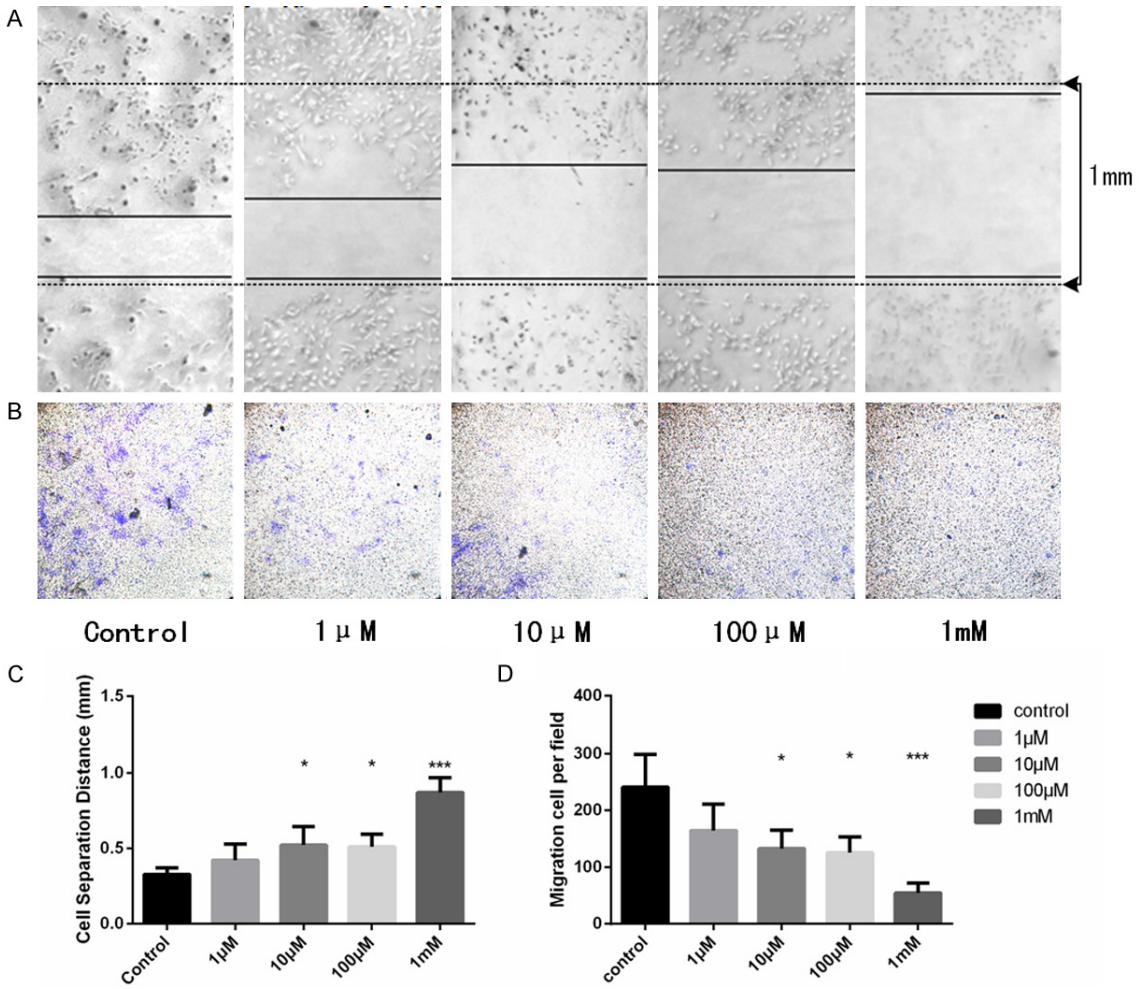

Figure 3. Cell migration detected by the scratch test (magnification, × 100) and Transwell migration assay (magnification, × 100). A. Scratch tests showed that BMSCs migration distance to wound indicated with 1 mm scratch pen. B. Transwell migration assay showed the number of migrated BMSCs decreased compared to that in the control group. C. Shows the statistical analysis of the separation distance of cells in all groups. D. Shows the statistical analysis of the migrated cells per field in all groups. These indicated that 10 μM, 100 μM, and 1 mM concertation of nicotine inhibited the migration of BMSCs in vitro ($P < 0.05$). Data shown are the means ± SD for 3 independent experiments. *$P < 0.05$, ***$P < 0.001$ compared to the control group treated without nicotine.

with 10 mM nicotine showed significantly decreased viability ($P < 0.001$; **Figure 2A**). For assessing the differentiation, BMSCs were treated with osteoblast-induction stimulants and various concentrations of nicotine (1 μM-1 mM) for 21 days, and Alizarin red assay was performed (**Figure 2B**, **2C**). Calcium accumulation was strongly observed in the Control BMSCs (0.613 ± 0.085), and the accumulation did not show significant change when BMSCs were treated with nicotine at the concentrations from 1 μM to 100 μM (all $P < 0.05$). However, the differentiation was significantly Inhibited at 1 mM ($P < 0.05$; **Figure 2D**).

Effect of nicotine on migration of BMSCs in vitro

In order to determine whether nicotine influenced the migration of BMSCs, a scratch test and a Transwell assay was developed for 24 h. As shown in **Figure 3A**, the scratch assay results indicated that after treated with nicotine, migration rate of BMSCs was decreased as compared with that in control group at 10 μM, 100 μM, and 1 mM (all $P < 0.05$), while the differences of migration rate between control group and 1 μM showed no significance ($P = 0.354$ **Figure 3C**). Transwell assay results dem-

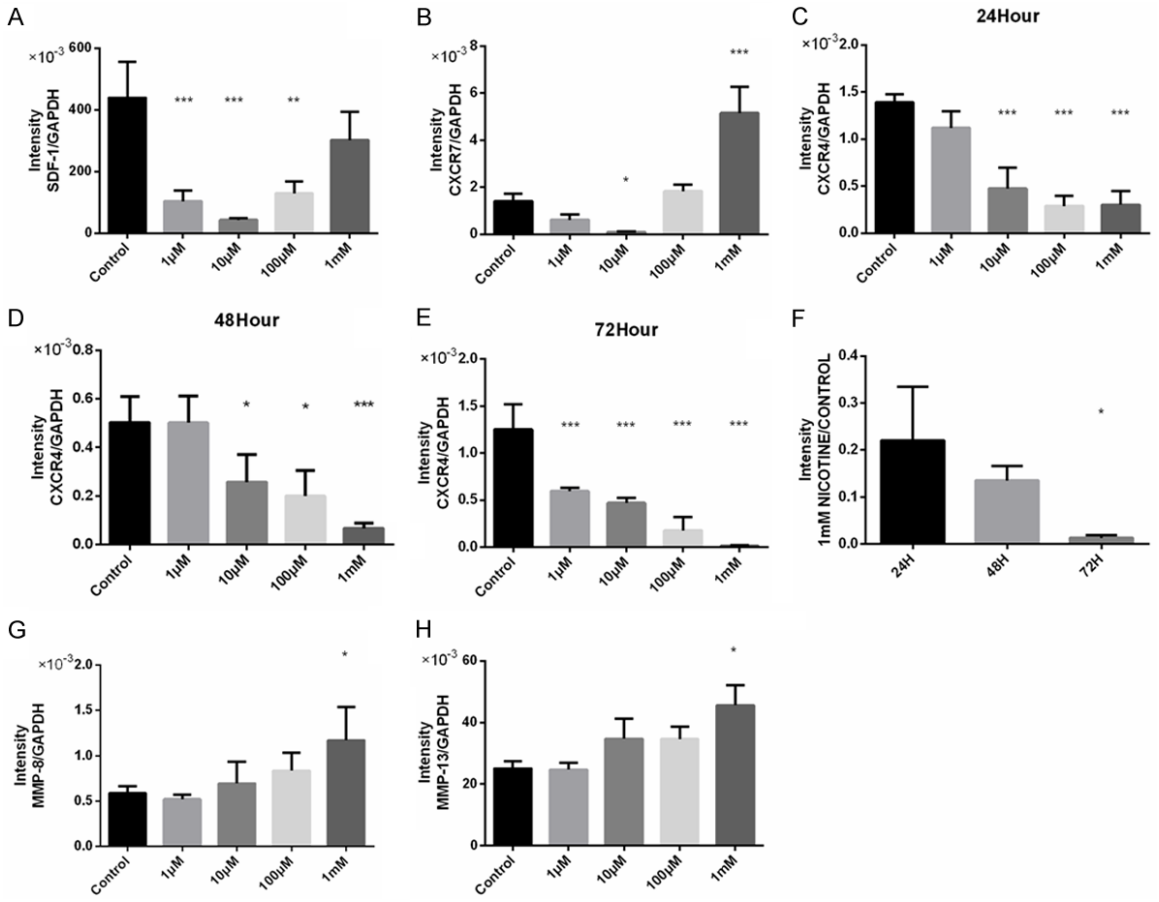

Figure 4. Effect of nicotine on the gene expression levels of migration markers. Osteoblasts and BMSCs were incubated in the presence of 1 μM-1 mM of nicotine for appropriate time. Transcription levels of SDF-1 on Osteoblasts, CXCR4, CXCR7, MMP-8 and MMP-13 on BMSCs were determined by Realtime-quantitative PCR. A. Expression of SDF-1 in untreated osteoblasts (controls) and in cells treated with 1 μM-1 mM nicotine for 24 hours. Results are expressed as fold-change in GAPDH normalized mRNA values. B. Expression of CXCR7 in BMSCs with or without nicotine for 24 hours. GAPDH was used as the reference. C-E. Expression of CXCR4 in BMSCs for 24 hours, 48 hours or 72 hours. GAPDH was used as the reference. F. The ratio of CXCR4 expression between 1 mM treated group and control group in 24-72 hours. G, H. Expression of MMP-8 and MMP-13 in BMSCs with or without nicotine for 48 hours. GAPDH was used as the reference. Data shown are the means ± SD for 3 independent experiments. *$P < 0.05$, **$P < 0.05$, ***$P < 0.001$ compared to the control group treated without nicotine.

onstrated a similar outcome that all concertation except 1 μM ($P = 0.1094$) showed significance Inhibitory effect on BMSCs migration between control group and nicotine group (all $P < 0.05$).

Effect of nicotine on mRNA expression

Osteoblasts (MC3T3-E1) and BMSCs were incubated in the presence of 1 μM-1 mM of nicotine for appropriate time. Transcription levels of SDF-1 on Osteoblasts, CXCR4, CXCR7, MMP-8 and MMP-13 on BMSCs were determined by Realtime-quantitative PCR. Results are expressed as fold-change in GAPDH normalized mRNA values. Treatment of Osteoblasts with 1 μM-100 μM of nicotine resulted in significant lower expression levels of SDF-1 in Osteoblasts ($P < 0.05$) while 1 mM did not show no significant effect (**Figure 4A**). The expression of CXCR7 in BMSCs was significantly inhibited by nicotine at the concentrations of 1 μM but promoted by 1 mM ($P < 0.05$ **Figure 4B**). Then, compared to the control, those treated with 10 μM-1 mM of nicotine showed remarkedly reduced expression levels of CXCR4 from 24 hours to 72 hours. The 1 μM nicotine group did not show obvious down regulation relative to control group until 72 hours ($P < 0.05$ **Figure 4C-E**). **Figure 4F** indicated that the expression of CXCR4 in BMSC treated with 1 mM nicotine exhibited a downward trend in comparison to control group from 24

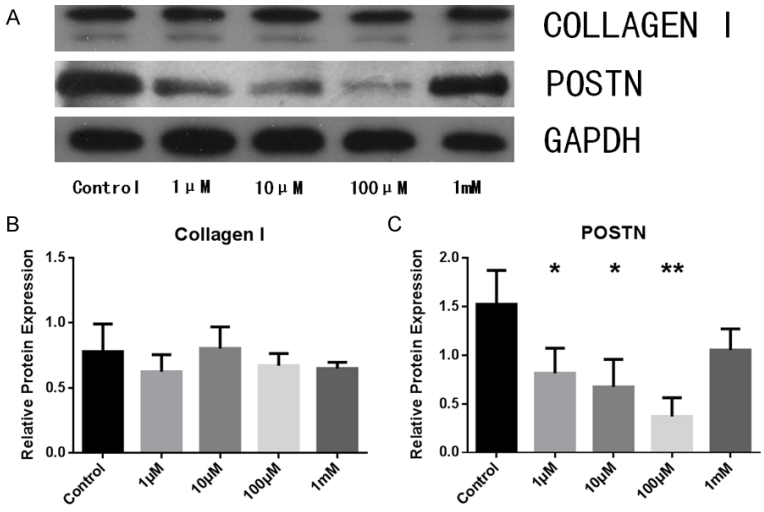

Figure 5. Effect of nicotine on the protein expression levels of Osteoblasts ECM in the presence of 1 μM-1 mM of nicotine for 7 days detected by western blot. A. Western blot results showed that in Osteoblasts, Collagen I was not significantly altered by nicotine but POSTN protein expression in the 1 μM-100 μM nicotine group was lower than that in the control group. GAPDH was used as the reference. B, C. Shows the statistical analysis of the western blot in all groups. Data shown are the means ± SD for 3 independent experiments. *P < 0.05, **P < 0.05 compared to the control group treated without nicotine.

h to 72 h as a function of time (**Figure 4F**). Treatment of BMSCs with 1 Mm-100 μM of nicotine did not result in any significant difference in MMP-8, MMP-13 but with 1 mM of nicotine both of them were upregulated (P < 0.05, **Figure 4G**, **4H**).

Effect of nicotine on osteoblasts ECM expression

Osteoblasts were incubated in the presence of 1 μM-1 mM of nicotine for 7 days. Postn were significantly inhibited in 1 μM-100 μM nicotine group (all P < 0.05), while no difference of protein levels existed between 1 mM nicotine group and the control (P = 0.6425) (**Figure 5A**, **5C**). At the same time, no difference of protein levels of collagen I existed (**Figure 5B**).

Interaction between BMSCs and osteoblasts

To emulate how Osteoblasts in the niche can attract BMSCs, we cultured femur derived living and devitalized bone segments with GFP-BMSCs for 7 days. The middle femur bone segments (5 mm), without bone marrow, were cut longitudinally to expose the medullary side. After 7 days, Cells were fixed and restained by DAPI. A large number of GFP+ cells accumulated and adhered around the bone segment (**Figure 6A-C**), while little GFP+ cells gathered around the devitalized bone segments (**Figure 6D-F**). When 100 μM nicotine was applied, little GFP+ cells gathered around the living bone segments (**Figure 6G-I**).

BMSCs homing to fracture in vivo

Test A and control A were used in vivo small animals imaging 7 days post-surgery and sacrificed for histological examination sequently. The amount of GFP+ cells the section from mice treated with nicotine dramatically less than that in control groups (**Figure 7A**, **7B**, **7E**, P < 0.05). Furthermore, the result of in vivo small animals imaging technology also shown the same outcome (**Figure 7C**, **7D**).

Micro-CT analysis

Micro-CT analysis was performed to evaluate the healing progresses of defects at 2 and 5 weeks, respectively. The 3D reconstruction images of μ-CT showed that the healing of control group was dramatically better than those of the nicotine groups at 2 weeks postoperatively. Setting the defect area as area of interest, quantitative data of μ-CT showed that control group was significantly higher than the control bone volume/tissue volume (BV/TV **Figure 8C**). However, no great difference was observed at 5 weeks (**Figure 8A-C**).

Discussion

Cigarette smoke consists of more than 4000 chemical substances which, nicotine is the main component [28]. In vitro and in vivo experiments have been conducted to investigate that nicotine delays fracture healing [11, 29, 30]. However, the mechanism through which nicotine affects bone healing remains unclear. In vitro studies employ various concentrations of nicotine, ranging from 0.01 μM to 50 mM [11]. Previous reports revealed that exposure to high concentrations of nicotine (as high as 5 mM) can damage the proliferation and mineralization capacity of BMSCs [12]. But low nico-

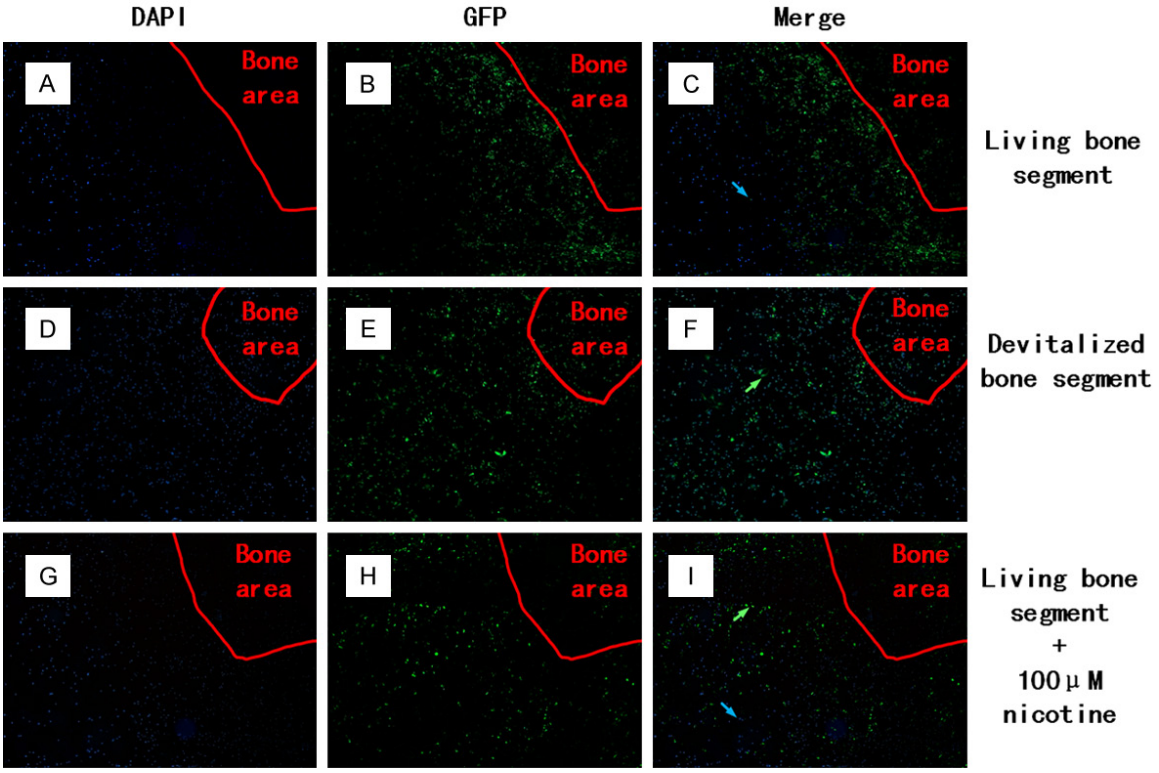

Figure 6. WT femur-derived bone segments without bone marrow were cultured with GPF-BMSCs (cells in green) for 7 days (magnification, × 100). Red line represents the bone edge. Blue indicated the cell nucleus which were re-stained by DAPI. Blue arrows indicated GPF negative cells from wild type C57BL/6 mice bone segment. Green and green arrows indicated GPF-BMSCs. A-C. Living bone segments cultured with GPF-BMSCs. D-F. Devitalized bone segments cultured with GPF-BMSCs. G-I. Living bone segments cultured with GPF-BMSCs at nicotine concentration of 100 μM.

tine concentration leads to bone healing delay but does not significantly affect the expression of bmp-2 and the radio density of bone regeneration [31]. We speculate that sub-toxic clinical concentration of nicotine might affect fracture healing in other mechanisms. According to clinical epidemiological investigation, the blood levels of nicotine obtained from habitual cigarette smokers range from 0.06 to 1.2 mM and, the level of nicotine in the saliva has been reported to be 0.6-9.6 mM [32]. In the present study, nicotine concentrations, ranging from 1 μM to 10 mM, were carefully selected to correspond to the levels in blood and saliva of smokers. However, since treatment with 10 mM nicotine induced extensive cell death, we ranged the concertation from 1 μM to 1 mM (**Figure 2A**). Osteoblasts and the precursor cells BMSCs are key cells involved in bone regeneration. Bone healing can be delayed by suppressing the recruitment of BMSCs to the bone segmental defect [33]. Osteoblasts, as the most important cells of bone healing, can secrete chemokines to promote the homing of BMSCs. Regulation of SDF-1 production by osteoblasts could be a possible mechanism underlying stem cell homing [34]. Few in vitro studies have examined the effects of nicotine on the migration and homing of BMSCs. In the present study, we investigated if delayed bone healing could be attributed to the inhibition of osteoblasts induction of BMSC homing and migration by nicotine.

Cell proliferation determines the amount of BMSCs that have generative effect in the body. In the present study, BMSCs were cultured in medium containing different concentrations of nicotine for 7 days. After 7 days, a stimulating effect was observed in cells treated with 1 mM nicotine. Treatment with 10 mM nicotine dramatically decreased cell proliferation and led to cell death (on the first day). Hence, nicotine, depending on exposure conditions (time and concentrations), inhibited or stimulated cell proliferation (bimodal effect);

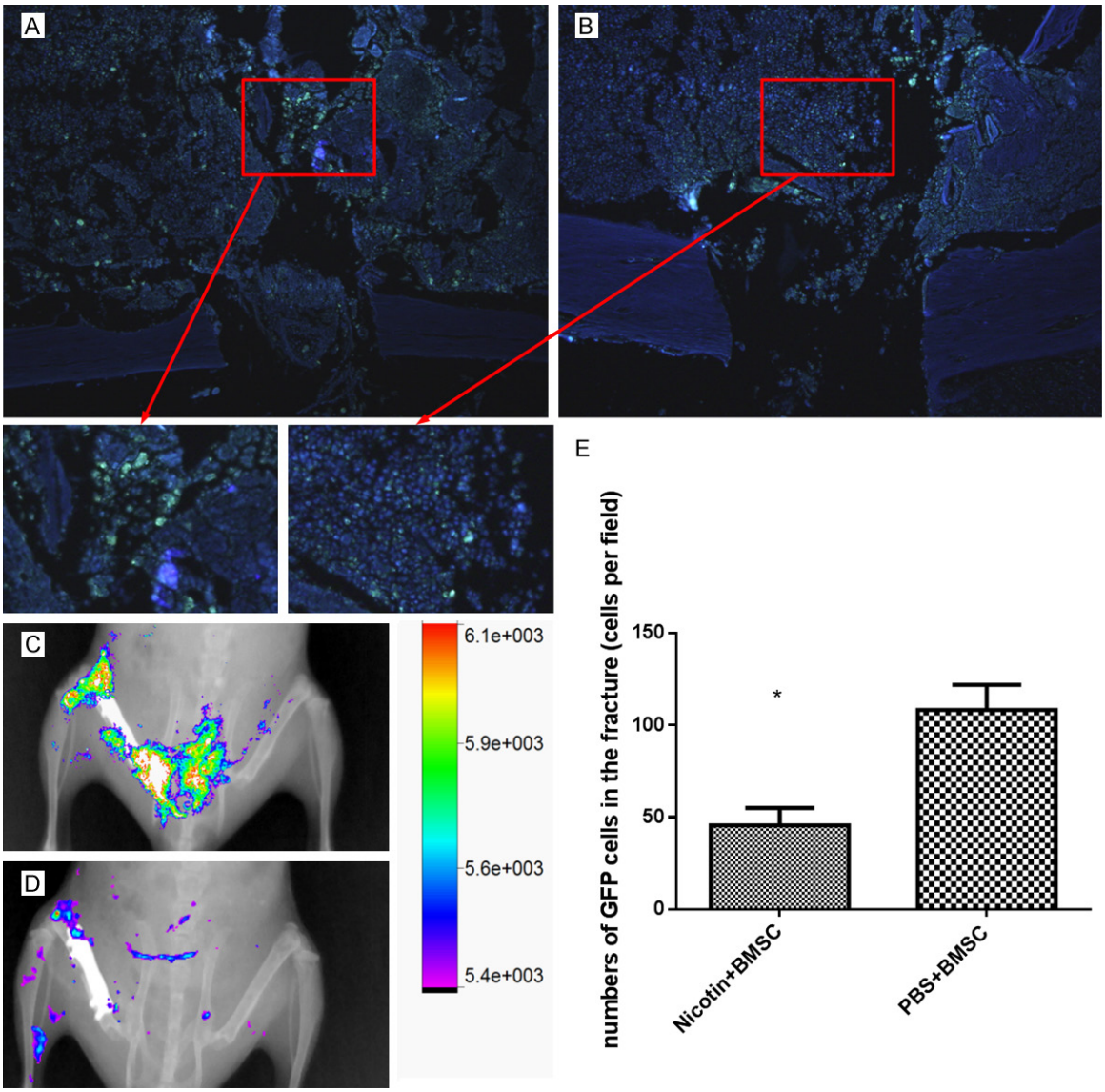

Figure 7. BMSCs homing to fracture detected by dissection specimens and in vivo small animals imaging technology after surgery for 7 days. (A, B) Immunofluorescence with an anti-GFP antibody was performed to detect GPF+ BMSCs (cells in green) from control group (A) or nicotine group with subcutaneous injection of 2 μg nicotine per day for one mouse (B) in longitudinal section (magnification, × 100). (C, D) Injected GPF-BMSC visualized with Small Animal Imaging Technology. Intensity of fluorescence signal around the fracture site from control group (C) was dramatical stronger than nicotine treated group (D) (2 μg/mouse/day). (E) Shows the statistical analysis of the immunofluorescence dissection in both groups. Data shown are the means ± SD for 6 independent specimens. *P < 0.05, **P < 0.05 compared to the control group treated without nicotine.

this finding is similar to those previously reported (Kamer et al., 2006; Rothem et al., 2009; Kim et al., 2012) [12, 35, 36]. Treatment with 1 mM nicotine considerably stimulated cell proliferation and led to cell death on the 7th day (**Figure 2A**). At this concentration, nicotine not only inhibited calcium accumulation (**Figure 2B-D**) but also significantly stimulated the proliferation of osteoblasts while no significant alteration to controls. Determining if the proliferation of osteoblasts is inhibited by nicotine and eventually leads to delayed fracture healing remains difficult.

Stem cell differentiation into tissue-specific cells is one of the mechanisms for stem cell repair at injury sites during healing [37]. Cigarette inhibits the osteogenic differentiation of human osteoprogenitor cells, and nicotine reduces the osteogenic differentiation of BM-

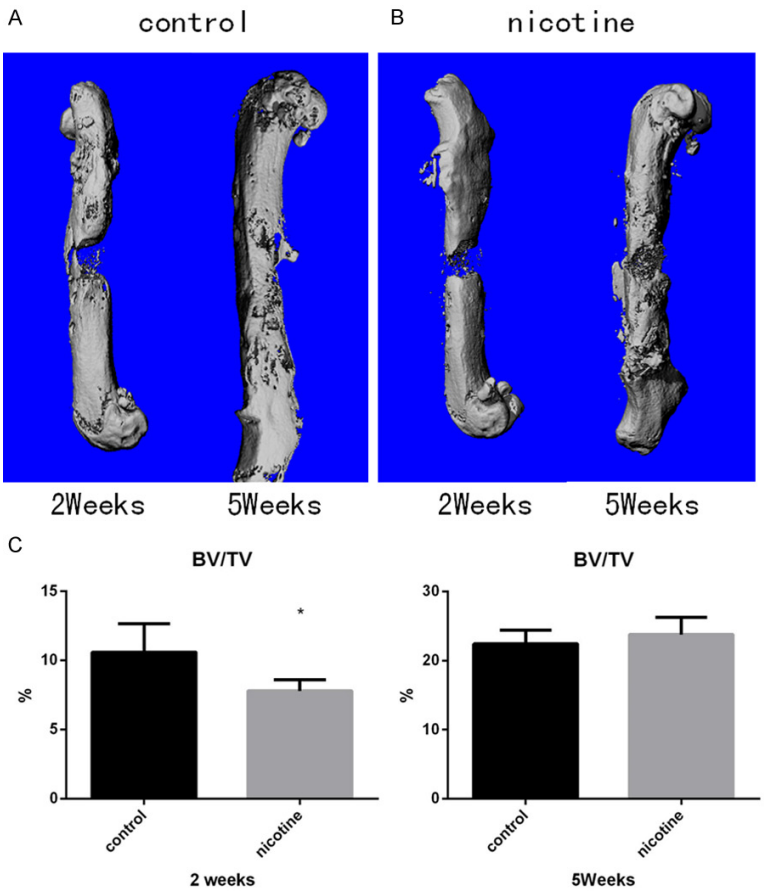

Figure 8. Micro-CT images and analysis showed the defect healing of nicotine group was delayed than control group. A. Micro-CT images of defect healing femurs of control group at 2 and 5 weeks. B. Micro-CT images of defect healing femurs of nicotine group (2 μg/mouse/day) at 2 and 5 weeks. C. Quantification data of the defect area (*P < 0.05 n = 6).

SCs. The culture medium was changed every 3 days with varied concentrations of nicotine to simulate continuous exposure through daily use of cigarette. The present study showed that there was no statistical difference of calcium deposition can be found in BMSCs after inducing osteogenic differentiation at low doses of nicotine. Nodule formation was significantly reduced when the cells were cultured with 1 mM nicotine (**Figure 2B-D**). Nicotine could affect the differentiation potential of BMSCs only at such a high concentration which was found in the peak level of heavy smoker lasting for a short time might not be related to delayed healing clinically [38].

Cell homing has rationality and good prospects in bone regeneration; as such, promoting stem cell homing, whether from local area, systemic circulation, or both, could be an important strategy for bone healing. Scratch test and Transwell chamber test were conducted to examine the effects of nicotine on BMSC homing in vivo. According to the results, nicotine significantly inhibited the migration of BMSCs. Based on previous reports, inhibition of BMSCs migration lead to the fracture healing disorder [33], so we suspected that this might be an important cause for the effect of nicotine on fracture healing. Increasing lines of evidence indicate that SDF-1 and its cellular receptor, CXCR4 and CXCR7 play an important role in BMSC migration [39]. SDF-1/CXCR4/CXCR7 promotes the migration of stem cells associated with injury repair in many species and tissue types [40-42]. Moreover, the expression levels of SDF-1 and CXCR4 were predominantly increased under hypoxic conditions, such as acute injury [43]. Osteoblasts are the most important source of SDF-1 in the skeleton; moreover, itself was an important factor to attract the BM-SCs homing [44]. In our experiments, we found that, the segments of bone attached with living Osteoblasts could attract BMSCs and the tendency was inhibited by nicotine, it the amount of SDF-1 secreted by osteoblasts decreased at several nicotine concentrations (**Figure 4**). Furthermore, CXCR4/CXCR7 expression was significantly reduced by treatment with nicotine showing a significant dose and time dependence trend. On the contrary, the important impact of invasion, MMP-8 and MMP-13 [24, 25], remained stable at all concentration of nicotine.

Matricellular proteins play a pivotal role in tissue homeostasis and in different pathological processes. Type I collagen was an important components in tendon, bone and skin which co-localizes and interacts with periostin by which increased the proliferation and migration rates of different cells, such as fibroblasts

or osteoblast-like cells [45, 46]. The high expression of periostin promotes the migration and proliferation of BMSCs but not in bone differentiation [45]. In the present study, Postn was decreased by low levels of nicotine, while there was non-significant on collagen I. The reduced expression of Postn might suppress the migration of BMSCs.

Further, we used a femur fracture model to study the homing of fracture-directed BMSCs Since the transplanted BMSCs in C57 mice survived for 5-10 days only; as such, in vivo imaging was performed 7 days after the surgery [47]. We do not recommend injection of large amounts of BMSCs because it leads to massive pulmonary infarction and redistribution in the liver, bone marrow and other organs [48]. In the bone marrow cavity of other bones and liver, we can still find some signals, but the major signals were concentrated in the fracture area; therefore, the experimental scheme selected was considered feasible (**Figure 7C**, **7D**). The fluorescence signal of EGFP was tracked by histological examination either. The signal at the fracture site was weaken in the nicotine treated group both in in vivo imaging and histological examination (**Figure 7**). Hence, nicotine prevented BMSCs from moving towards the fracture area.

Mineralized callus volume quantified by micro-CT surface rendering of the mineral component is useful for investigating bony bridging across the fracture site to detected bone healing delay [49]. In the nicotine group models, MV/CV was significantly lower in 2 weeks compared with the PBS control group, but in the 5 week, there was no significant difference between the two groups (**Figure 8C**). According to our previous research, the segmental bone defect in the femur could be healed well at 5 weeks after the operation [21]. Therefore, we indicated that the fracture healing of the mice in the nicotine group was delayed, but not lead to definite negative impact on the final union, which is similar to the result in clinical practices [50].

The obtained data suggests the possible mechanism of low levels of nicotine in inducing bone healing delay. Under the “normal” nicotine blood concentrations in smokers, the proliferation and osteogenesis of osteoblasts may not be significantly affected. The obvious inhibition of migration and homing in vivo and in vivo demonstrates that nicotine may influence bone metabolism and formation. Hence, smoking may be an important risk factor for bone healing because it causes nonunion and delayed healing. Although the proposed mechanism could be explained by the down-regulation of SDF-1/CXCR4/CXCR7 and Postn, further investigation must be performed.

Acknowledgements

This work was supported by the Natural Science Foundation of China (No.81470718 and No.81771051).

Disclosure of conflict of interest

None.

Address correspondence to: Zubing Li, State Key Laboratory Breeding Base of Basic Science of Stomatology (Hubei-MOST) and Key Laboratory of Oral Biomedicine, Ministry of Education, School and Hospital of Stomatology and Department of Oral and Maxillofacial Trauma and Plastic Surgery, Wuhan University Stomatological Hospital, Wuhan University, Wuhan 430079, Hubei, China. Tel: 0086 18186133585; Fax: 86-027-87686217; E-mail: lizubing@whu.edu.cn

References

[1] Iribarren C, Tekawa IS, Sidney S and Friedman GD. Effect of cigar smoking on the risk of cardiovascular disease, chronic obstructive pulmonary disease, and cancer in men. N Engl J Med 1999; 340: 1773-1780.

[2] Liu Y, Gao J, Shou J, Xia H, Shen Y, Zhu S and Pan Z. The prevalence of cigarette smoking among rural-to-urban migrants in China: a systematic review and meta-analysis. Subst Use Misuse 2016; 51: 206-215.

[3] Li Q, Hsia J and Yang G. Prevalence of smoking in China in 2010. N Engl J Med 2011; 364: 2469-2470.

[4] Liu S, Zhang M, Yang L, Li Y, Wang L, Huang Z, Wang L, Chen Z and Zhou M. Prevalence and patterns of tobacco smoking among Chinese adult men and women: findings of the 2010 national smoking survey. J Epidemiol Community Health 2017; 71: 154-161.

[5] Patel RA, Wilson RF, Patel PA and Palmer RM. The effect of smoking on bone healing: a systematic review. Bone Joint Res 2013; 2: 102-111.

[6] Scolaro JA, Schenker ML, Yannascoli S, Baldwin K, Mehta S and Ahn J. Cigarette smoking increases complications following fracture: a systematic review. J Bone Joint Surg Am 2014; 96: 674-681.
[7] Sarmiento A and Latta LL. Randomized trial of reamed and unreamed intramedullary nailing of tibial shaft fractures. J Bone Joint Surg Am 2009; 91: 1274; author reply 1274-1275.
[8] Truntzer J, Vopat B, Feldstein M and Matityahu A. Smoking cessation and bone healing: optimal cessation timing. Eur J Orthop Surg Traumatol 2015; 25: 211-215.
[9] Sloan A, Hussain I, Maqsood M, Eremin O and El-Sheemy M. The effects of smoking on fracture healing. Surgeon 2010; 8: 111-116.
[10] Zheng LW, Ma L and Cheung LK. Changes in blood perfusion and bone healing induced by nicotine during distraction osteogenesis. Bone 2008; 43: 355-361.
[11] Kallala R, Barrow J, Graham SM, Kanakaris N and Giannoudis PV. The in vitro and in vivo effects of nicotine on bone, bone cells and fracture repair. Expert Opin Drug Saf 2013; 12: 209-233.
[12] Kim BS, Kim SJ, Kim HJ, Lee SJ, Park YJ, Lee J and You HK. Effects of nicotine on proliferation and osteoblast differentiation in human alveolar bone marrow-derived mesenchymal stem cells. Life Sci 2012; 90: 109-115.
[13] Gullihorn L, Karpman R and Lippiello L. Differential effects of nicotine and smoke condensate on bone cell metabolic activity. J Orthop Trauma 2005; 19: 17-22.
[14] Zhang W, Zhu C, Wu Y, Ye D, Wang S, Zou D, Zhang X, Kaplan DL and Jiang X. VEGF and BMP-2 promote bone regeneration by facilitating bone marrow stem cell homing and differentiation. Eur Cell Mater 2014; 27: 1-11; discussion 11-12.
[15] Prockop DJ. Marrow stromal cells as stem cells for nonhematopoietic tissues. Science 1997; 276: 71-74.
[16] Rifas L, Arackal S and Weitzmann MN. Inflammatory T cells rapidly induce differentiation of human bone marrow stromal cells into mature osteoblasts. J Cell Biochem 2003; 88: 650-659.
[17] Derubeis AR and Cancedda R. Bone marrow stromal cells (BMSCs) in bone engineering: limitations and recent advances. Ann Biomed Eng 2004; 32: 160-165.
[18] Sangani R, Pandya CD, Bhattacharyya MH, Periyasamy-Thandavan S, Chutkan N, Markand S, Hill WD, Hamrick M, Isales C and Fulzele S. Knockdown of SVCT2 impairs in-vitro cell attachment, migration and wound healing in bone marrow stromal cells. Stem Cell Res 2014; 12: 354-363.
[19] de Almeida TF, Romana-Souza B, Machado S, Abreu-Villaca Y and Monte-Alto-Costa A. Nicotine affects cutaneous wound healing in stressed mice. Exp Dermatol 2013; 22: 524-529.
[20] Cheng G, Li Z, Wan Q, Lv K, Li D, Xing X and Li Z. A novel animal model treated with tooth extraction to repair the full-thickness defects in the mandible of rabbits. J Surg Res 2015; 194: 706-716.
[21] Huang X, Li Y, Xu J, Liu K, Yu X, Cheng X, Xu D and Li Z. Restoration of murine femoral segmental defect using CTGF-overexpressing MC3T3-E1 cells. Am J Transl Res 2016; 8: 1530-1540.
[22] Liu HB, Liu SB, Li Y, Wang XH, Xue WJ, Ge GQ and Luo XH. The role of SDF-1-CXCR4/CXCR7 Axis in the therapeutic effects of hypoxia-preconditioned mesenchymal stem cells for renal ischemia/reperfusion injury. PLoS One 2012; 7.
[23] Cai Y, Li X, Wang YS, Shi YY, Ye Z, Yang GD, Dou GR, Hou HY, Yang N, Cao XR and Lu ZF. Hyperglycemia promotes vasculogenesis in choroidal neovascularization in diabetic mice by stimulating VEGF and SDF-1 expression in retinal pigment epithelial cells. Exp Eye Res 2014; 123: 87-96.
[24] Nygardas PT and Hinkkanen AE. Up-regulation of MMP-8 and MMP-9 activity in the BALB/c mouse spinal cord correlates with the severity of experimental autoimmune encephalomyelitis. Clin Exp Immunol 2002; 128: 245-254.
[25] Hattori N, Mochizuki S, Kishi K, Nakajima T, Takaishi H, D'Armiento J and Okada Y. MMP-13 plays a role in keratinocyte migration, angiogenesis, and contraction in mouse skin wound healing. Am J Pathol 2009; 175: 533-546.
[26] Saito Y, Sato S, Oginuma T, Saito Y, Arai Y and Ito K. Effects of nicotine on guided bone augmentation in rat calvarium. Clin Oral Implants Res 2013; 24: 531-535.
[27] Yu ZL, Li DQ, Huang XY, Xing X, Yu RQ, Li Z and Li ZB. Lysophosphatidic acid upregulates connective tissue growth factor expression in osteoblasts through the GPCR/PKC and PKA pathways. Int J Mol Med 2016; 37: 468-474.
[28] Horinouchi T, Higashi T, Mazaki Y and Miwa S. Carbonyl compounds in the gas phase of cigarette mainstream smoke and their pharmacological properties. Biol Pharm Bull 2016; 39: 909-914.
[29] Law MR and Hackshaw AK. A meta-analysis of cigarette smoking, bone mineral density and risk of hip fracture: recognition of a major effect. BMJ 1997; 315: 841-846.
[30] Hoogendoorn JM, Simmermacher RK, Schellekens PP and van der Werken C. [Adverse ef-

fects if smoking on healing of bones and soft tissues]. Unfallchirurg 2002; 105: 76-81.
[31] Ma L, Sham MH, Zheng LW and Cheung LK. Influence of low-dose nicotine on bone healing. J Trauma 2011; 70: E117-121.
[32] Benowitz NL. Drug therapy. Pharmacologic aspects of cigarette smoking and nicotine addiction. N Engl J Med 1988; 319: 1318-1330.
[33] Xu QC, Hao PJ, Yu XB, Chen SL, Yu MJ, Zhang J and Yang PS. Hyperlipidemia compromises homing efficiency of systemically transplanted BMSCs and inhibits bone regeneration. Int J Clin Exp Pathol 2014; 7: 1580-1587.
[34] Jung Y, Wang J, Schneider A, Sun YX, Koh-Paige AJ, Osman NI, McCauley LK and Taichman RS. Regulation of SDF-1 (CXCL12) production by osteoblasts; a possible mechanism for stem cell homing. Bone 2006; 38: 497-508.
[35] Kamer AR, El-Ghorab N, Marzec N, Margarone JE 3rd and Dziak R. Nicotine induced proliferation and cytokine release in osteoblastic cells. Int J Mol Med 2006; 17: 121-127.
[36] Rothem DE, Rothem L, Dahan A, Eliakim R and Soudry M. Nicotinic modulation of gene expression in osteoblast cells, MG-63. Bone 2011; 48: 903-909.
[37] Morsczeck C, Schmalz G, Reichert TE, Vollner F, Galler K and Driemel O. Somatic stem cells for regenerative dentistry. Clin Oral Investig 2008; 12: 113-118.
[38] Benowitz NL. Pharmacologic aspects of cigarette-smoking and nicotine addiction. N Engl J Med 1988; 319: 1318-1330.
[39] Kucia M, Ratajczak J, Reca R, Janowska-Wieczorek A and Ratajczak MZ. Tissue-specific muscle, neural and liver stem/progenitor cells reside in the bone marrow, respond to an SDF-1 gradient and are mobilized into peripheral blood during stress and tissue injury. Blood Cells Mol Dis 2004; 32: 52-57.
[40] Li Q, Zhang A, Tao C, Li X and Jin P. The role of SDF-1-CXCR4/CXCR7 axis in biological behaviors of adipose tissue-derived mesenchymal stem cells in vitro. Biochem Biophys Res Commun 2013; 441: 675-680.
[41] Wang Y, Fu W, Zhang S, He X, Liu Z, Gao D and Xu T. CXCR-7 receptor promotes SDF-1alpha-induced migration of bone marrow mesenchymal stem cells in the transient cerebral ischemia/reperfusion rat hippocampus. Brain Res 2014; 1575: 78-86.
[42] Periyasamy-Thandavan S, Herberg S, Arounleut P, Upadhyay S, Dukes A, Davis C, Johnson M, McGee-Lawrence M, Hamrick MW, Isales CM and Hill WD. Caloric restriction and the adipokine leptin alter the SDF-1 signaling axis in bone marrow and in bone marrow derived mesenchymal stem cells. Mol Cell Endocrinol 2015; 410: 64-72.
[43] Li J, Guo W, Xiong M, Han H, Chen J, Mao D, Tang B, Yu H and Zeng Y. Effect of SDF-1/CXCR4 axis on the migration of transplanted bone mesenchymal stem cells mobilized by erythropoietin toward lesion sites following spinal cord injury. Int J Mol Med 2015; 36: 1205-1214.
[44] Yu L, Tu Q, Han Q, Zhang L, Sui L, Zheng L, Meng S, Tang Y, Xuan D, Zhang J, Murray D, Shen Q, Cheng J, Kim SH, Dong LQ, Valverde P, Cao X and Chen J. Adiponectin regulates bone marrow mesenchymal stem cell niche through a unique signal transduction pathway: an approach for treating bone disease in diabetes. Stem Cells 2015; 33: 240-252.
[45] Soikkeli J, Podlasz P, Yin M, Nummela P, Jahkola T, Virolainen S, Krogerus L, Heikkila P, von Smitten K, Saksela O and Holtta E. Metastatic outgrowth encompasses COL-I, FN1, and POSTN up-regulation and assembly to fibrillar networks regulating cell adhesion, migration, and growth. Am J Pathol 2010; 177: 387-403.
[46] Le Lous M, Allain JC, Cohen-Solal L and Maroteaux P. Hydrothermal isometric tension curves from different connective tissues. Role of collagen genetic types and noncollagenous components. Connect Tissue Res 1983; 11: 199-206.
[47] Everaert BR, Bergwerf I, De Vocht N, Ponsaerts P, Van Der Linden A, Timmermans JP and Vrints CJ. Multimodal in vivo imaging reveals limited allograft survival, intrapulmonary cell trapping and minimal evidence for ischemia-directed BMSC homing. BMC Biotechnol 2012; 12: 93.
[48] Iwai S, Sakonju I, Okano S, Teratani T, Kasahara N, Yokote S, Yokoo T and Kobayash E. Impact of ex vivo administration of mesenchymal stem cells on the function of kidney grafts from cardiac death donors in rat. Transplant Proc 2014; 46: 1578-1584.
[49] Dickson GR, Geddis C, Fazzalari N, Marsh D and Parkinson I. Microcomputed tomography imaging in a rat model of delayed union/nonunion fracture. J Orthop Res 2008; 26: 729-736.
[50] Adams CI, Keating JF and Court-Brown CM. Cigarette smoking and open tibial fractures. Injury 2001; 32: 61-65.